Quantum complementarity of cavity photons coupled to a three-level system

R. Vilardi,[1] A. Ridolfo,[1,2] S. Portolan,[3] S. Savasta,[1] and O. Di Stefano[1,*]

[1]*Dipartimento di Fisica della Materia e Ingegneria Elettronica, Università di Messina, Salita Sperone 31, I-98166 Messina, Italy*

[2]*Technische Universität München, Physik Department, I James-Franck-Strasse, D-85748 Garching, Germany*

[3]*Institut Néel-CNRS, 25 Avenue des Martyrs, BP 166, F-38042 Grenoble Cedex 9, France*

(Received 2 August 2011; published 20 December 2011)

Recently a device enabling the ultrafast all-optical control of the wave-particle duality of light was proposed [Ridolfo *et al.*, Phys. Rev. Lett. **106**, 013601 (2011)]. It is constituted by a three-level quantum emitter strongly coupled to a microcavity and can be realized by exploiting a great variety of systems ranging from atomic physics and semiconductor quantum dots to intersubband polaritons and Cooper pair boxes. Control pulses with specific arrival times, performing which-path and quantum-eraser operations, are able to destroy and recover interference almost instantaneously. Here we show that the coherence sudden death implies the sudden birth of a higher order correlation function storing coherence. Such storing enables coherence rebirth after the arrival of an additional suitable control pulse. We derive analytical calculations describing the all-optical control of the wave-particle duality and the entanglement-induced switch-off of the strong coupling regime. We also present analytical calculations describing a homodynelike method exploiting pairs of phase locked pulses with precise arrival times to probe the optical control of wave-particle duality of this system. Within such a method the optical control of wave-particle duality can be directly probed by just detecting the photons escaping the microcavity.

DOI: 10.1103/PhysRevA.84.063842 PACS number(s): 42.50.Pq, 71.36.+c, 42.50.Dv

I. INTRODUCTION

In quantum science and quantum engineering it is highly desirable to control the interaction between single photons and individual optical emitters [1–3]. It is possible to modify photon fields around an emitter using high-finesse optical cavities. Quantum emitters (QEs) in a microcavity (MC) can absorb and spontaneously re-emit a photon many times before dissipation becomes effective and a mixed light-matter eigenmode regime arises [1,4–8]. Recently ultrafast switch-on of the strong coupling regime has been achieved by exploiting intersubband transitions in quantum wells [9]. In addition, the all-optical time control of the strong coupling (switch-on and -off) between a single cascade three-level QE and a MC has been demonstrated theoretically [10]. It was found that only specific arrival times of the control pulses succeed in switching off the Rabi oscillations. When switch-off fails, the control pulse may be exploited to suddenly destroy first-order coherence of cavity photons without affecting their strong coupling population dynamics. Such behavior can be fully understood as a manifestation of quantum complementarity [11]. In this case the induced entanglement between the cavity and the QE enables the latter to store the which-way information on photon paths, hence destroying coherence according to the quantum complementarity principle [11]. However, the loss of coherence is not irreversible, being that the which-path detector is itself a quantum system (quantum marker) [12]. A further suitable control pulse is able to suddenly erase the which-way information, thus inducing the sudden rebirth of coherence. This scheme enables all-optical which-path and quantum-eraser operations, able to suddenly switch off and switch on first-order coherence of cavity photons. Such operations are generally performed by changing some part of the experimental apparatus, or by changing the detected observables [11–15].

The rebirth of coherence opens the question where information on the phase gets stored after the switch-off of first-order coherence. In this paper we investigate by numerical and analytical calculations the system coherences, finding where the lost phase information gets stored before the possible rebirth. Moreover, by employing some reasonable approximations, we calculate analytically the time evolution of the system quantum state. Analytical results enable a detailed understanding of the intriguing physics of the all-optical control of wave-particle duality of cavity photons. Coherence switching on and off of cavity photons in the strong coupling regime can be probed experimentally by employing pairs of phase locked pulses with precise arrival times and by simply detecting photons escaping through a cavity mirror. Here we present analytical calculations describing this kind of phase-sensitive experiment.

II. THEORETICAL MODEL

Here we present the model describing the all-optical scheme for the ultrafast time control of the strong coupling between the emitter and the cavity. The three-level emitter in a ladder configuration embedded in a semiconductor MC is sketched in Fig. 1. $|s\rangle$ is a QD state at lower energy the transition between the states $|g\rangle$ and $|e\rangle$ is resonantly coupled with the MC resonance.

The Hamiltonian describing the cavity embedded cascade three-level system reads

$$H = H_0 + H_{\rm I} + H_{\rm in}, \tag{1}$$

where

$$H_0 = \sum_{j={\rm g,e}} \omega_j \sigma_{j,j} + \omega_{\rm c} a^\dagger a \tag{2}$$

*omar.distefano@unime.it

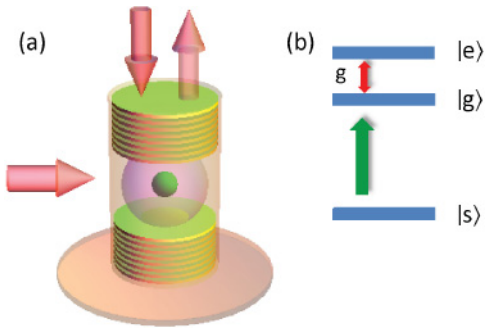

FIG. 1. (Color online) (a) Schematic setup to implement the all-optical control of the strong coupling regime; (b) the relevant level structure of the QE coupled to the resonator.

is the free Hamiltonian of the two separated system,

$$H_{\mathrm{I}} = g\sigma_{\mathrm{g,e}}a^{\dagger} + \mathrm{H.c.} \tag{3}$$

is the QE-MC interaction Hamiltonian in the rotating wave approximation, and

$$H_{\mathrm{in}} = \epsilon_{\mathrm{p}}^{*}(t)a + \epsilon_{\mathrm{c}}^{*}(t)\sigma_{\mathrm{s,g}} + \mathrm{H.c.} \tag{4}$$

describes both the influence of the driving control pulses $\epsilon_{\mathrm{c}}(t)$ directly coupled to the QE and of the coherent probe pulses $\epsilon_{\mathrm{p}}(t)$ feeding the MC. Here a denotes the destruction operator for the cavity mode and $\sigma_{\alpha,\beta} \equiv |\alpha\rangle\langle\beta|$ describes the transition or projection operators involving the levels of the QE [see Fig. 1(b)]. We consider Gaussian ultrafast pulses at frequencies centered at ω_{g} and $\omega_{\mathrm{a}} = \omega_{\mathrm{e}} - \omega_{\mathrm{g}}$, respectively. Losses can be taken into account introducing the system density matrix ρ. It obeys a quantum master equation in the Born-Markov approximation expressed in the usual Lindblad form [10,16]. The Markovian interaction with reservoirs determining the decay rates for the QE exciton and the cavity mode is described by the following usual Liouvillian terms:

$$\mathcal{L}\rho = -\frac{1}{2}\sum_{\mu}(L_{\mu}^{\dagger}L_{\mu}\rho + \rho L_{\mu}^{\dagger}L_{\mu} - 2L_{\mu}\rho L_{\mu}^{\dagger}), \tag{5}$$

where the Lindblad operators L_{μ} describe the various scattering channels. The decay terms $\mathrm{e} \to \mathrm{g}$ are described by $L_{\mathrm{e}\to\mathrm{g}} = \sqrt{\gamma_{\mathrm{e}}}\,|\mathrm{g}\rangle\langle\mathrm{e}|$, $L_{\mathrm{g}\to\mathrm{s}} = \sqrt{\gamma_{g}}\,|\mathrm{s}\rangle\langle\mathrm{g}|$, and the cavity decay term is $L_{a} = \sqrt{\gamma_{\mathrm{a}}}a$. The master equation for the density operator of the cavity emitter can be written as

$$\frac{\partial\rho}{\partial t} = i[\rho, H] + \mathcal{L}\rho, \tag{6}$$

with the Hamiltonian and the Liouvillian given by Eqs. (1)–(5). Starting from the master equation, we derive the coupled equations of motion for the cavity-photon and exciton populations, coherences, and higher order correlation functions, which we solve numerically by representing the photon operators on a basis of Fock number states. We start studying the switch-on of vacuum Rabi oscillations.

Figure 2 compares the strong coupling dynamics of photonic populations (i.e., the expectation value of the intracavity photon number $\langle a^{\dagger}a\rangle$) with its coherent part $|\langle a\rangle|^2$. At initial time, the cavity is in the vacuum state and the QE in its ground state $|s\rangle$. Then, control π pulse (green higher pulse in Fig. 2) is sent ($\gamma_{\mathrm{a}}t = 8 \times 10^{-2}$) resonant with the transition $|s\rangle \leftrightarrow |g\rangle$

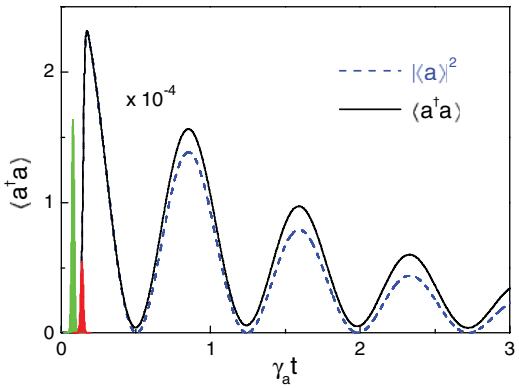

FIG. 2. (Color online) Cavity-photon population (continuous line) and its coherent part (dashed line) displaying Rabi oscillations; the Gaussian probe (solid lower line) and control (solid higher line) pulses are also sketched (their displayed time width and relative amplitudes do not correspond to their actual values).

populating level $|g\rangle$. After such pulse, a weaker probe beam resonant both with the cavity mode and the transition $|g\rangle \leftrightarrow |s\rangle$ feeds the cavity (red lower pulse in Fig. 2; $\gamma_{\mathrm{a}}t = 14 \times 10^{-2}$). Almost instantaneously vacuum Rabi oscillations appear. We consider a weak Gaussian input field feeding the cavity ($\omega_{\mathrm{p}} = \omega_{\mathrm{g}} - \omega_{\mathrm{s}}$) with pulse area $\ll 1$:

$$\epsilon_{\mathrm{p}}(t) = A_{\mathrm{p}}\exp(-i\omega_{\mathrm{p}}t)\,\exp\left[-\frac{(t-t_1)^2}{2\sigma_{\mathrm{p}}^2}\right], \tag{7}$$

and a Gaussian control pulse with pulse area π exciting directly the QE:

$$\epsilon_{\mathrm{c}}(t) = A_{\mathrm{c}}\exp(-i\omega_{\mathrm{c}}t)\,\exp\left[-\frac{(t-t_{\mathrm{c}})^2}{2\sigma_{\mathrm{c}}^2}\right]. \tag{8}$$

Calculations have been carried out by using $g = 85\ \mu\mathrm{eV}$, $\gamma_{\mathrm{a}} = 20\ \mu\mathrm{eV}$, $\gamma_{\mathrm{g}} = 2\ \mu\mathrm{eV}$, $\gamma_{\mathrm{e}} = 5\ \mu\mathrm{eV}$, $\omega_{\mathrm{g}} = 1.329\ \mathrm{eV}$, $\omega_{\mathrm{e}} - 2\omega_{\mathrm{g}} = -2.28$ meV, $\sigma_{\mathrm{p}} = \sigma_{\mathrm{c}} = 0.124\gamma_{\mathrm{a}}$. Despite the absence of pure dephasing, a non-negligible loss of coherence of the photon field after the switch-on is evident [10].

In Ref. [10] it has been shown that an additional π control pulse at a Rabi maximum, almost instantaneously induces the transition from strong to weak coupling. In this way a full time control of the QE-MC strong interaction can be achieved. Here we concentrate on the full time control of the wave-particle behavior of cavity photons. In the next section [see Fig. 3(a)] we will show the impact of an additional π control pulse sent at the Rabi minimum: The intensity of Rabi oscillations carries on almost undisturbed, while its previously dominating coherent part suddenly disappears ($\langle a\rangle \simeq 0$), suggesting the emergence of particlelike behavior. Such striking dependence of the dynamics on the arrival time of the control pulse can be explained taking into account the quantum state describing the system when the cavity is fed by a low-intensity pulse (probe) [10]. More specifically, depending on the arrival times of control pulses, a variety of exotic nonadiabatic cavity quantum electrodynamics effects can be observed. Control pulses with specific arrival times, performing which-path and quantum-eraser operations, are able to suddenly switch off and on first-order coherence of cavity photons, without affecting their strong coupling population dynamics.

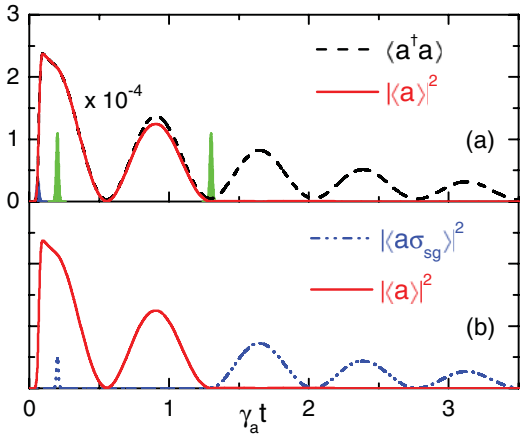

FIG. 3. (Color online) (a) Dynamics of the cavity-photon population $\langle a^\dagger a\rangle$ (dashed line) and of the square modulus of its coherent part (continuous line) $|\langle a\rangle|^2$ in the presence of two π control pulses (higher solid lines); the second control pulse is sent at a minimum of $\langle a^\dagger a\rangle$. Panel (b) displays the square modulus of the mixed MC-QE coherence $|\langle a\sigma_{sg}\rangle|^2$ together with $|\langle a\rangle|^2$. The sudden vanishing of first-order coherence after the arrival of the second control pulses coincides with the birth of the higher order coherence $\langle a\sigma_{sg}\rangle$.

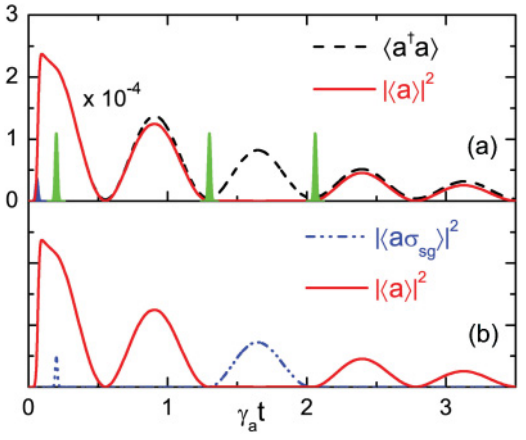

FIG. 4. (Color online) (a) Dynamics of cavity-photon population (continuous line) and its coherent part (dashed line) in the presence of three control pulses. The second and third control pulses arrive at cavity-photon population minima. The second control pulse induces a sudden vanishing of coherence without affecting the cavity-photon population; the arrival of the third pulse induces the complete recovering of coherence. (b) Displays the square modulus of the mixed MC-QE coherence $|\langle a\sigma_{sg}\rangle|^2$ together with $|\langle a\rangle|^2$. The sudden vanishing of first-order coherence after the arrival of the second control pulses coincides with the birth of the higher order coherence $\langle a\sigma_{sg}\rangle$; the arrival of the third pulse causes the inverse process.

III. OPTICAL CONTROL OF WAVE-PARTICLE DUALITY

In this section, we develop theoretical calculations for the all-optical control of the wave-particle duality and the entanglement-induced switch-off of the strong coupling regime. A detailed analysis of the dynamics of the cavity-photon population when different opportunely delayed control pulses are sent inside the structure is presented. We will show how the first-order correlation is totally erased when the second control pulse excites the system at a cavity-field minimum [see Fig. 3(a)]. Nevertheless, as pointed out also in Ref. [10] [see also Fig. 4(a)], such coherence sudden death is not irreversible. In order to analyze in detail such reversibility and to study where the coherence is stored in the system, we present exact numerical calculations. In addition, in order to have at the same time both a more deep understanding and a simple picture of the physics underlying such phenomena, a detailed analytical study of the quantum dynamics of the MC-QE state is required.

The physical mechanisms allowing the switch-off and switch-on of the first-order coherence and the birth of higher order cavity-QE coherences can be explained taking into account the approximate quantum state describing the system when the cavity is fed by a low-intensity pulse (probe). Starting from the operator master equation [Eq. (6)], considering only a coherent excitation (zero temperature reservoirs), and retaining up to one cavity-photon states, it is possible to show that the density operator factorizes in the form [17] $\rho(t) = |\psi(t)\rangle\langle\psi(t)|$. The general quantum state $|\psi(t)\rangle$ after the arrival of the probe and of the first control pulse can be developed as

$$|\psi(t)\rangle = c_g(t)|1\rangle|g\rangle + d(t)|0\rangle|g\rangle + c_e(t)|0\rangle|e\rangle, \qquad (9)$$

where, in the tensorial ket product $|\cdot\rangle|\cdot\rangle$, the first ket describes the photon number state and the second the QE state. We employ the following assumptions and approximations: (i) We consider only probe pulses with pulse area much lower than one; (ii) we also consider fast control and probe pulses with $\sigma_p, \sigma_c \ll g$; (iii) we neglect the decay rate of level g; (iv) in addition, for the sake of simplicity, we assume that the decay rate of cavity photons be equal to that of level e: $\gamma_a = \gamma_e$. With all the above assumptions, and taking as $t = 0$ the arrival time of the probe pulse, the coefficients describing the dynamics of the quantum state (9) acquire the simple form:

$$c_g(t) = a_p \cos(\Omega t/2)\exp[-\gamma t/2],$$
$$c_e(t) = a_p \sin(\Omega t/2)\exp[-\gamma t/2];$$

with $a_p \ll 1$ and $d(t) \approx 1$, where $a_p \propto A_p$ describes the pulse area.

In the subsequent subsections, we will show in detail how the dynamics of the system strongly depends on the control pulse arrival time and also how the coherence is transferred among different correlation functions. We answer the question of where the information is stored about coherence when we observe the sudden death of first-order coherence and, after sending an opportune control beam inside the cavity, its sudden rebirth. In particular, we present both the exact numerical calculations and the approximate quantum state analysis. Hence we present a detailed analysis of the quantum dynamics of the MC-QE state in the presence of three control pulses.

A. Where coherence goes

In Ref. [10] it has been shown that the coherence sudden death is not irreversible [see also Fig. 4(a)]. First-order coherence, destroyed after the arrival of the π control pulse at the Rabi minimum (particlelike behavior), can be recovered (wavelike behavior) after the arrival of a further π control

pulse at a subsequent Rabi minimum. Such reversibility raises the question where information on the phase gets stored in the quantum system. In this section we explore such a question, showing that actually the sudden death of first-order coherence induces a complementary birth of a high-order photon-emitter correlation function. This analysis allows one to better understand the rebirth of coherence after the arrival of a further suitable control pulse [10].

The dynamics of the cavity-photon population, as well as that of its coherent part $|\langle a\rangle|^2$ in the presence of two π control pulses, is shown in Fig. 3(a). A second control pulse is sent inside the structure at a minimum of the cavity population. It is evident how the first-order correlation is totally erased when the second control pulse excites the system at a cavity-field minimum. On the contrary the population of cavity photons is unaffected by the second pulse. In order to better understand the effects of the arrival of the second pulse, it is useful to investigate higher order coherences. We focus the attention on the second-order coherence between the photon and quantum emitter s-g transition $\langle a\sigma_{\rm sg}\rangle$. In particular, its square modulus $|\langle a\sigma_{\rm sg}\rangle|^2$ is displayed in Fig. 3(b). Its complementary behavior with respect to the square modulus of the first-order correlation function $|\langle a\rangle|^2$ is evident: When the latter disappears, the sudden birth of the first one can be observed. By a direct comparison of Figs. 2 and 3, we observe that the sum of the two correlations square moduli calculated when the second control pulse is sent inside the cavity (see Fig. 3) is equal to the square modulus of the first-order correlation calculated in the absence of the second pulse (see Fig. 2).

In Fig. 4, the dynamics of the cavity-photon population and its coherent part in the presence of three control pulses are displayed. We start analyzing the physical situation where the second and third control pulses both arrive at cavity-photon population minima. As just shown in Fig. 3 and as is also clear from Fig. 4(a), the arrival of the second control pulse at a cavity-photon minimum causes the switch-off of first-order coherence. Figure 4 shows that the arrival of a third control pulse at the next minimum of cavity photons induces an instantaneous rebirth of coherence. We conclude that it is possible to obtain a complete switching control over first-order photonic coherence. The complementary behavior of $|\langle a\sigma_{\rm sg}\rangle|^2$ is displayed in Fig. 4(b). We observe that the lost (or more appropriately hidden) coherence caused by the arrival of the second control pulse is instantaneously transferred from the first-order correlation to the second one. Then, the third control pulse arrival activates the inverse process and first-order correlation is recovered, while second-order coherence erases.

We now study the process just discussed exploiting the dynamics of the approximate quantum state. From Eq. (9) the resulting first-order coherence, in the absence of subsequent control pulses, can be easily obtained:

$$\begin{aligned}\langle\psi(t)|a|\psi(t)\rangle &= d^*(t)c_{\rm g}(t)\langle 0|a|1\rangle\langle {\rm g}|{\rm g}\rangle = d^*(t)c_{\rm g}(t)\\ &\approx c_{\rm g}(t) = a_{\rm p}\cos(\Omega t/2)e^{-\frac{\gamma}{2}t}.\end{aligned} \tag{10}$$

Analogously, we can calculate the expectation value for the second-order coherence. We obtain

$$\langle\psi(t)|a\sigma_{\rm sg}|\psi(t)\rangle = d^*(t)c_{\rm g}(t)\langle {\rm g}|\sigma_{\rm sg}|{\rm g}\rangle\langle 0|a|1\rangle = 0, \tag{11}$$

in agreement with the numerical results presented above. At a cavity minimum ($t = t_{\rm m}$), we have $c_{\rm g}(t_{\rm m}) \approx 0$ and $c_{\rm e}(t_{\rm m}) = a_{\rm p}$ is maximum (i.e., the cavity photon is absorbed by the QE that jumps to the excited state $|{\rm e}\rangle$). After the arrival of the second control pulse, implying the transition $|{\rm g}\rangle \to |{\rm s}\rangle$, the state $|\psi(t_{\rm m}^-)\rangle$ becomes $|\psi(t_{\rm m}^+)\rangle = d(t_{\rm m}^+)|0\rangle|{\rm s}\rangle + c_{\rm e}(t_{\rm m}^+)|0\rangle|{\rm e}\rangle$. During the free evolution of the state ($t > t_{\rm m}$), the emission of a cavity photon by the QE associated with the transition $|{\rm e}\rangle \to |{\rm g}\rangle$ is allowed and the state evolves into

$$|\psi(t)\rangle = c_{\rm g}(t)|1\rangle|{\rm g}\rangle + d(t)|0\rangle|{\rm s}\rangle + c_{\rm e}(t)|0\rangle|{\rm e}\rangle \quad \text{for} \quad t > t_{\rm m}. \tag{12}$$

It is straightforward to obtain for the first-order coherence at $t > t_{\rm m}$:

$$\begin{aligned}&\langle\psi(t)|a|\psi(t)\rangle\\ &\quad = [d^*(t)c_{\rm g}(t)\langle {\rm s}|{\rm g}\rangle + c_{\rm e}^*(t)c_{\rm g}(t)\langle {\rm e}|{\rm g}\rangle]\langle 0|a|1\rangle = 0.\end{aligned} \tag{13}$$

This result explains the coherence sudden death observed in the numerical calculations discussed in this subsection: First-order coherence goes to zero owing to the orthogonality of the different QE quantum states. In contrast, the expectation value for the second-order correlation is given by

$$\begin{aligned}\langle\psi(t)|a\sigma_{\rm sg}|\psi(t)\rangle &= d^*(t)c_{\rm g}(t)\langle {\rm s}|\sigma_{\rm sg}|{\rm g}\rangle\langle 0|a|1\rangle = d^*(t)c_{\rm g}(t)\\ &\approx c_{\rm g}(t) = a_{\rm p}\cos(\Omega t/2)e^{-\frac{\gamma}{2}t}.\end{aligned} \tag{14}$$

It gets the same value of $\langle\psi(t)|a|\psi(t)\rangle$ calculated in the absence of the second pulse [see Eq. (10)] in agreement with numerical results displayed in Fig. 4. Hence, the process inducing the sudden death of the first-order correlation also allows for the coherence total transfer to the second-order cavity-QE correlation $\langle a\sigma_{\rm sg}\rangle$. The present quantum state analysis (before the arrival of a third control pulse) explains the corresponding results displayed in Figs. 3 and 4.

B. Quantum dynamics of the microcavity—quantum emitter state

In this subsection, we analyze the case where the second control pulse arrives at a cavity-photon population minimum, while the third is sent at a maximum. The cavity-photon population and its coherent part are displayed in Fig. 5(a). The first control pulse induces a strong population inversion from level $|{\rm s}\rangle$ to level $|{\rm g}\rangle$ (switch-on of coupling). The second control pulse excites the system at a cavity-field minimum (i.e., a minimum in the photon Rabi oscillations) inducing the erasure of first-order coherence, while the QE-MC system remains in the strong coupling regime. Sending a third control pulse at a maximum of cavity-photon population induces an apparent transition to the weak coupling regime where the cavity-photon population decays exponentially [see Fig. 5(a)]. The origin of the transition will become clear in the next section after the analytical study of the quantum dynamics. In Fig. 5(b), both the dynamics of the coherent part of the photon populations and the square modulus of the second-order photon-QE coherence $|\langle a\sigma_{\rm sg}\rangle|^2$ are shown. Also in this case the complementary behavior between this second-order correlation and the first one is evident. We also observe that the arrival of the third control pulse, differently from the previous case (see Fig. 4), is not able to restore

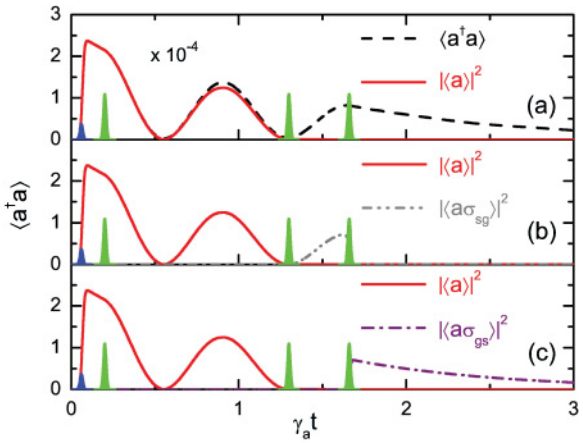

FIG. 5. (Color online) Dynamics of the cavity-photon population and square moduli of coherences in the presence of three control pulses. The second and third control pulses arrive at a cavity-photon population minimum and maximum, respectively. (a) Cavity-photon population (dashed black line) and its coherent part (continuous red line). After the arrival of the second control pulse we observe the sudden vanishing of $|\langle a\rangle|^2$ and after the arrival of the third pulse we observe the sudden transition from the vacuum Rabi oscillations of the cavity-photon population to the exponential decay. (b) Coherent part of cavity-photon population $|\langle a\rangle|^2$ and the square modulus of the mixed MC-QE coherence $|\langle a\sigma_{sg}\rangle|^2$. The latter springs up at the arrival of the second pulse and disappears at the arrival of the third pulse. (c) Square modulus of the mixed MC-QE coherence $|\langle a\sigma_{gs}\rangle|^2$ associated with the g-s transition; it springs up at the arrival of the third pulse.

first-order coherence. In addition it induces the sudden death of the higher order coherence $\langle a\sigma_{sg}\rangle$. The question arises as to where the coherence has been transferred in the present case. Figure 5(c) provides the answer. It display the calculated second-order coherence between photon and quantum emitter g-s transition $\langle a\sigma_{gs}\rangle$. We observe that the value assumed by the g-s second-order correlation is zero before the arrival of the third control pulse. Then we assist to its sudden birth.

In order to better understand these effects, we now study the process exploiting the dynamics of the approximate quantum state shown in Eq. (9). After the arrival of the second pulse, the quantum state is described by Eq. (12). At a cavity maximum $= c_e(t) \approx 0$ and we have

$$|\psi(t)\rangle = c_g(t)|1\rangle|g\rangle + d(t)|0\rangle|s\rangle.$$

The third π control pulse sent at such a maximum (see Fig. 5) induces the $|g\rangle \leftrightarrow |s\rangle$ QE-state transitions. Hence, indicating with t_{mM} the arrival time of the third pulse, the state of the QE-MC system results in

$$|\psi(t_{mM}^{+})\rangle = c_g(t_{mM})|1\rangle|s\rangle + d(t_{mM})|0\rangle|g\rangle. \quad (15)$$

For $t > t_{mM}$ the state maintains the same structure because transitions $|g\rangle \rightarrow |e\rangle$ are not allowed because state $|g\rangle$ in Eq. (15) is associated with a zero-cavity-photon state. Hence no oscillations in the cavity-photon population can be observed. For $t > t_{mM}$, the quantum state is

$$|\psi(t)\rangle = c_g(t)|1\rangle|s\rangle + d(t)|0\rangle|g\rangle, \quad (16)$$

where now $c_g(t) = a_p \exp[-\gamma t/2]$. The resulting first-order coherence for $t > t_{mM}$ can be calculated as follows:

$$\langle\psi(t)|a|\psi(t)\rangle = d^*(t)c_g(t)\langle g|s\rangle\langle 0|a|1\rangle = 0, \quad (17)$$

and the s-g second-order coherence results in

$$\langle\psi(t)|a\sigma_{sg}|\psi(t)\rangle = d^*(t)c_g(t)\langle 1|a|0\rangle\langle s|\sigma_{sg}|g\rangle = 0. \quad (18)$$

Our analysis explains the erasure of both first- and second-order s-g coherences. We may question where the information on the phase is stored. As observed in Fig. 5(c), after the arrival of the third control pulse the second-order g-s correlation $\langle\psi(t)|a\sigma_{gs}|\psi(t)\rangle$ suddenly appears. In fact, it results as equal to zero until the third control pulse is sent in the structure as can be easily calculated. We thus obtain for $t > t_{mM}$,

$$\langle\psi(t)|a\sigma_{gs}|\psi(t)\rangle = d^*(t)c_g(t)\langle 0|a|1\rangle\langle g|\sigma_{gs}|s\rangle = d^*(t)c_g(t)$$
$$\approx c_g(t) = a_p e^{-\frac{\gamma}{2}t}. \quad (19)$$

We may conclude, in complete analogy with what was deduced above, that in this case the disappearance of both first-order and second-order s-g coherences induces a complementary appearance of an other second-order correlation where the role of the state $|s\rangle$ and $|g\rangle$ is exchanged. In addition, the value assumed by the g-s second-order correlation is the same assumed by the first-order correlation in the absence of the second and third control pulses [see Eqs. (10) and (19)] in agreement with numerical results shown in Fig. 5.

IV. HOW TO CHECK EXPERIMENTALLY THE ALL-OPTICAL CONTROL OF WAVE-PARTICLE DUALITY

Here we analyze in detail a recently proposed [18] simple implementation of a homodynelike method in order to check the coherence of cavity photons. The method can be implemented by feeding the MC with a pair of phase-locked probe pulses [19] and detecting the photons escaping the cavity. In this section we present detailed analytical calculations as well as additional numerical calculations providing a deeper understanding of the proposed detection scheme. It is worth noticing that the field amplitude $\langle a\rangle$ is not a physical observable and cannot directly be detected. Nevertheless $\langle a\rangle$ can be inferred via homodyne detection techniques. Calculations are carried out as in Ref. [10]. With respect to what was calculated and shown in Figs. 2 and 5 the probe field feeding the MC is now an overlap of the two delayed Gaussian pulses with a relative adjustable phase ϕ:

$$\epsilon_p(t) = A\exp(-i\omega_a t)\left\{\exp\left[-\frac{(t-t_1)^2}{(2\sigma^2)}\right]\right.$$
$$\left. + B\exp(i\phi)\exp\left[-\frac{(t-t_2)^2}{(2\sigma^2)}\right]\right\}. \quad (20)$$

Figure 6 displays the strong coupling dynamics obtained by this different cavity feeding. We used the same parameters adopted for the numerical results reported in the previous sections. The system is (i) initially excited by a π control pulse in order to invert the population between levels s and g, so that strong coupling can occur. Then (ii) a first probe

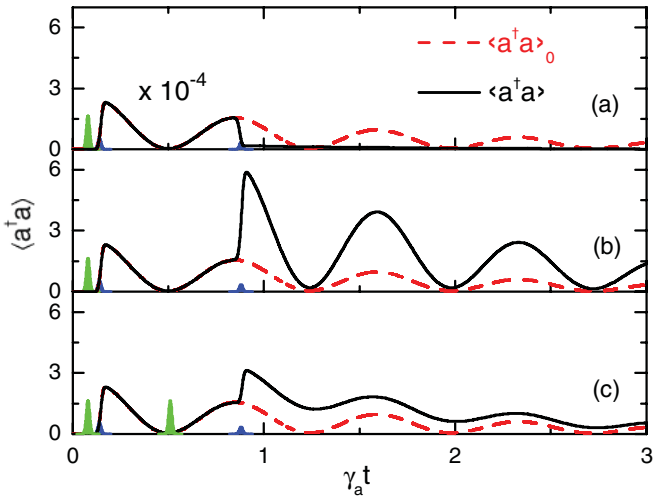

FIG. 6. (Color online) Cavity-photon populations in the presence of two phase-locked probe pulses and one (a) and (b) or two (c) control pulses. For comparison the cavity-photon population $\langle a^\dagger a\rangle_1$ when only a probe beam is sent (red dashed curve) is also shown. (a) Destructive interference after the arrival of a second phase-locked probe pulse with phase difference $\phi = 0$; (b) constructive interference after the arrival of a second phase-locked probe pulse with phase difference $\phi = \pi$; (c) absence of interference effects after sending a second control pulse at a cavity minimum (in this case only a small increase of the cavity-photon population due to additional photons entering in the cavity is observed).

pulse at $\gamma_a t_2 = 0.14$ (see the Gaussian blue lower solid curves) excites the MC determining the vacuum Rabi oscillations of the photonic population. Finally a second probe pulse (iii) excites the MC at the second Rabi maximum at $\gamma_a t_2 = 0.88$ and with $\phi = 0$. Almost complete destructive interference is observed. It is a signature of the expected coherence. It may be somewhat puzzling that, starting with a zero phase difference between the input pulses, destructive interference is achieved. This result is due to a specific property of vacuum Rabi oscillations (see, e.g., Ref. [20]) which need two Rabi periods in order to recover the initial phase. Sending the second probe pulse at the next Rabi maximum (here not shown) constructive interference can be found. The case of constructive interference when the second phase-locked probe pulses with phase difference $\phi = \pi$ is sent at the second Rabi maximum is shown in Fig. 6(b). Figure 6(c) differs from the situation in Fig. 6(a) for an additional control π pulse sent at the first Rabi minimum $\gamma_a t_2 = 0.49$, before the arrival of the second probe pulse. This second control pulse, as discussed in the previous sections, destroys almost instantaneously first-order optical coherence of cavity photons [see Fig. 3(a)]. Now the arrival of the second probe pulse just allows for a direct test of coherence. If cavity photons have actually lost their first-order coherence, the arrival of the second probe pulse will not give rise to interference effects. The small increment in the population observed in Fig. 4(c) is due to the augmented number of photons in the cavity which in this case is fed by two probe pulses. In addition, it is possible to show that such a result is independent on the relative phase ϕ (see also Fig. 9). Detection of this absence of interference would certify the coherence destruction predicted in Ref. [10] and shown in Fig. 5. In summary, the first control pulse gives

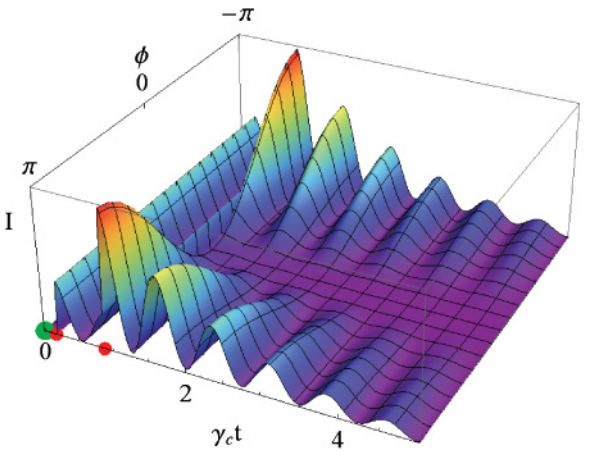

FIG. 7. (Color online) Cavity-photon populations as a function of time and of the phase difference ϕ between the two probe pulses. The second probe pulse is sent at the second cavity maximum. Interference is clearly visible. The arrival time of the control and probe pulses is indicated by the larger green (at $t = 0$) and smaller red disks.

rise to the strong coupling regime; the first probe beam can thus produce coherent vacuum Rabi oscillations; the optional additional control beam sent at a Rabi minimum will destroy the coherence of cavity photons generated by the first probe pulse; the second probe pulse will interfere with cavity photons only if they maintain their first-order coherence, hence it is able to test the coherence of cavity photons generated by the first probe pulse.

Figures 7–9 display cavity-photon populations as a function of time and of the relative phase ϕ between the two probe pulses. The arrival time of control (probe) pulses is indicated by larger green (smaller red) disks. The strong variation of $\langle a^\dagger a\rangle$ as a function of ϕ shown in Figs. 7 and 8 is clear evidence of interference effects due to the coherence of cavity photons. At the opposite Fig. 9(b), obtained sending the second probe pulse after a further control pulse at a Rabi minimum, shows no signal variation as a function of ϕ, a signature of the destroyed coherence.

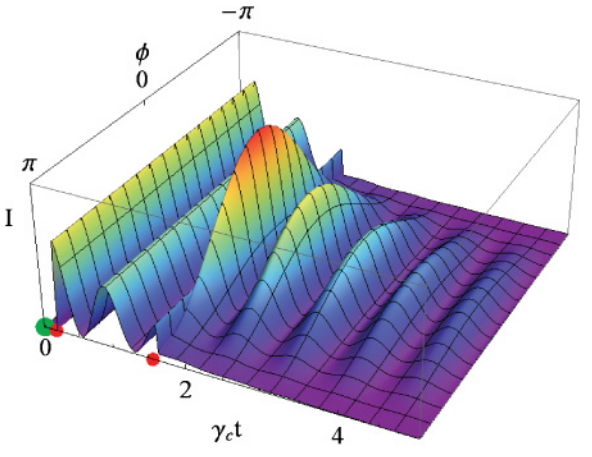

FIG. 8. (Color online) Cavity-photon populations as a function of time and of the phase difference ϕ between the two probe pulses. The second probe pulse is sent at the third cavity maximum. Interference effects are clearly visible.

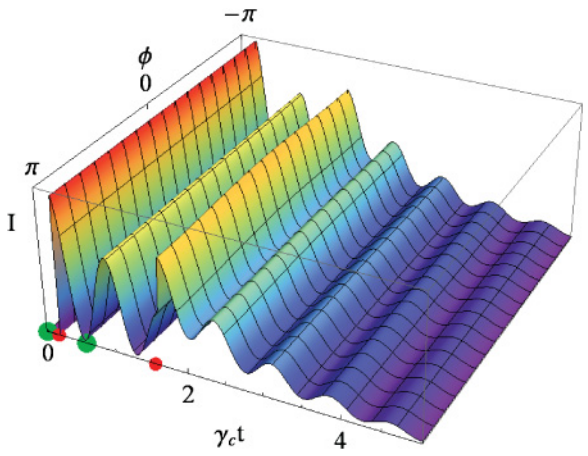

FIG. 9. (Color online) Cavity-photon populations as a function of time and of the phase difference between the two probe pulses ϕ. The second probe pulse is sent at the third cavity maximum after the arrival of a second π control pulse. The independence of the signal on ϕ certifies the absence of interference.

This peculiar behavior can be explained in terms of quantum complementarity as can be understood by analyzing the approximate quantum state. In the above-described homodynelike detection scheme, photons escaping the cavity are detected. Each detected photon comes from one of the two input coherent pulses. If there is no possibility, without perturbing the system, of gathering information on the origin (first or second input pulse) of the detected photon, according to the complementarity principle, wavelike behavior will emerge, and interference effects will be observed. On the contrary, if it is possible, even in principle to gather the which way information, interference effects will vanish and particlelike behavior emerges. Focusing our attention to the physical configuration described for Fig. 9, from Eq. (12) and remembering that the second probe pulse (at time $t = t_2$) is sent at a cavity population maximum ($c_e(t_2) \approx 0$), we have

$$|\psi(t_2^-)\rangle = c_g(t_2^-)|1\rangle|g\rangle + d(t_2^-)|0\rangle|s\rangle. \tag{21}$$

The second pump sent inside the cavity modifies the QE-MC wave-function evolution. The evolution operator may be developed up to the first order in the interaction as

$$U \simeq \mathbf{1} + b_p a^\dagger,$$

where $\mathbf{1}$ is the identity operator and $b_p \propto B_p \ll 1$ describes the pulse area of the second phase-locked probe pulse. Hence, the wave function becomes

$$\begin{aligned}|\psi(t_2^+)\rangle &= U|\psi(t_2^-)\rangle \\ &= c_g(t_2^+)|1\rangle|g\rangle + d(t_2^+)|0\rangle|s\rangle + d(t_2^+)b_p|1\rangle|s\rangle,\end{aligned} \tag{22}$$

where terms with more than one cavity-photon state are neglected. The wave function for $t > t_2$ evolves as

$$\begin{aligned}|\psi(t)\rangle &= c_g(t)|1\rangle|g\rangle + d(t)|0\rangle|s\rangle \\ &\quad + d(t)b_p e^{-\frac{\gamma}{2}t}|1\rangle|s\rangle + c_e(t)|0\rangle|e\rangle,\end{aligned} \tag{23}$$

We observe that, being $b_p = |b_p|\exp(i\phi)$ where ϕ is the relative phase of the second pulse, the information on ϕ is contained only in the coefficient of the state $|1\rangle|s\rangle$. This determines a possible which-path information. In particular, we are able to gather the which-way information of light emerging outside the cavity observing the QE state inside the cavity: If it is in its ground state $|g\rangle$, the light must originate from the first exciting probe (because no information about phase of the second pulse is contained in the coefficient of the state); on the contrary, if the QE results in the excited state $|s\rangle$, the light is due to the second probe exciting the cavity owing to the coefficient $\beta(t)b_p$. From Eq. (22), we can calculate the intensity of light $\mathcal{I} = \langle\psi(t)|a^\dagger a|\psi(t)\rangle$ detected outside the cavity:

$$\begin{aligned}\mathcal{I} &= |c_g(t)|^2 + |d(t)|^2|b_p|^2 e^{-\gamma t} \approx |c_g(t)|^2 + |b_p|^2 e^{-\gamma t} \\ &= e^{-\gamma t}[|a_p|^2\cos^2(\Omega t/2) + |b_p|^2],\end{aligned} \tag{24}$$

being $d(t) \approx 1$. It is clear that the light intensity detected is not affected by the phase difference between the two pulses exciting the cavity in agreement with numerical calculations displayed in Fig. 9. On the contrary, it is straightforward to find, by an analogous analytical calculation, that interference effects are present in the absence of the second control pulse.

This kind of experiment requires a thorough control over the time delay between the different optical pulses. Such a control is possible with modern time-resolved spectroscopy setups (see, e.g., Refs. [21] and [32]). One may also ask how to determine the precise timing of subsequent pulses from outside the cavity. One possible scheme consists into first sending only the first two pulses, namely the control beam and, after a small time delay (e.g., of the order of 1 ps), the probe pulse. In this case time-resolved detection of photons escaping the cavity will give an oscillating signal (S1) like the red-dashed curve in Fig. 6. The so obtained time-resolved S1 signal provides precise information on the needed arrival times of the next pulses. For example, in the situation of Fig. 7 we need to send an additional probe beam arriving inside the cavity at the Rabi maximum originating from the first probe pulse. At this stage, we switch off the first probe and send only one delayed probe beam. We will obtain a delayed oscillating signal (S2) which we can compare with S1. In particular comparing the time of the first maximum of S2 with the chosen maximum of S1, it is possible to determine the precise delay of the second pulse. It is also possible to repeat the second step with the adjusted delay in order to verify the correct timing. The situation described in Fig. 8 requires one additional control beam. In this case one possible timing scheme consists of sending only the probe beam as in Fig. 6 in the absence of the previous control beam. In this case the obtained signal will display an exponential decay. We can repeat the measurement sending after the probe a delayed control beam in order to gather information on the timing of the second control pulse. In this case we will observe the initial exponential decay followed by the sudden appearance of the Rabi oscillations (S3). The exact time of such appearance defines the arrival time inside the cavity of the control pulse. Comparing S3 with S1, it is possible to determine and tune the precise delay of the second control pulse.

V. CONCLUSIONS

The complementarity principle refers to the ability of quantum entities to behave as particles or waves under different experimental conditions. For example, in the famous double-slit experiment, a single electron can apparently pass through

both apertures simultaneously, forming an interference pattern. But if a "which-path" detector is employed to determine the particle's path, the interference pattern is destroyed. We carried out a detailed investigation of a recently proposed quantum device for the all-optical control of strong light matter interaction and wave-particle duality of photons [10]. We showed that the induced coherence sudden death implies the sudden birth of a higher order correlation function storing coherence. Such storing enables coherence rebirth after the arrival of an additional suitable control pulse. We also discussed a homodynelike method exploiting pairs of phase-locked pulses with precise arrival times, to probe the optical control of wave-particle duality of this system. Within such a method the optical control of wave-particle duality can be directly probed by just detecting the photons escaping the MC. We also presented approximate analytical calculations providing a deep understanding of the rich physics of this quantum device.

We hope that the intriguing effects here described will stimulate new experimental efforts. The analysis here developed can be applied to a quite large variety of state-of-the-art experiments and setups, ranging from atomic [22] and circuit-QED systems [23,24] and quantum dots in optical cavities [25] and can be extended to MC embedded quantum wells displaying intersubband polaritons [9] by exploiting the Heisenberg-Langevin method for interacting electron systems [26]. Generation and control of photonic quantum states from the microwave to the optical and THz regions can hence be studied on a common framework. In this light, the cavity embedded three-level cascade QE can be also exploited to study quantum phenomena in the ultrastrong coupling regime where counter-rotating light-matter terms become important and a wealth of forefront physical phenomena are conceivable [9,24,27,28]. Very recently a theoretical study beyond the rotating wave approximation of the dynamical Casimir emission from this system was reported [29]. Finally we observe that recently it was shown that ultracompact (with dimensions below the diffraction limit) hybrid structures, composed of metallic nanoparticles and a single quantum dot, can also achieve the strong coupling regime [30,31]. The all-optical control of light-matter interaction and of wave-particle duality can also be applied to these solid-state quantum plasmonic devices.

[1] J. M. Raimond, M. Brune, and S. Haroche, Rev. Mod. Phys. **73**, 565 (2001).

[2] C. Monroe, Nature (London) **416**, 238 (2002).

[3] L. M. Duan and H. J. Kimble, Phys. Rev. Lett. **92**, 127902 (2004).

[4] C. Weisbuch, M. Nishioka, A. Ishikawa, and Y. Arakawa, Phys. Rev. Lett. **69**, 3314 (1992).

[5] J. P. Reithmaier, G. Sek, A. Löffler, C. Hofmann, S. Kuhn, S. Reitzenstein, L. V. Keldysh, V. D. Kulakovskii, T. L. Reinecke, and A. Forchel, Nature (London) **432**, 197 (2004).

[6] T. Yoshie, A. Scherer, J. Hendrickson, G. Khitrova, H. M. Gibbs, G. Rupper, C. Ell, O. B. Shchekin, and D. G. Deppe, Nature (London) **432**, 200 (2004).

[7] K. Hennessy, A. Badolato, M. Winger, D. Gerace, M. Atatüre, S. Gulde, S. Fält, E. L. Hu, and A. Imamoglu, Nature **445**, 896 (2007).

[8] I. Chiorescu, P. Bertet, K. Semba, Y. Nakamura, C. J. P. M. Harmans, and J. E. Mooij, Nature (London) **431**, 159 (2004).

[9] G. Günter *et al.*, Nature (London) **458**, 178 (2009).

[10] A. Ridolfo, R. Vilardi, O. Di Stefano, S. Portolan, and S. Savasta, Phys. Rev. Lett. **106**, 013601 (2011).

[11] S. Dürr, T. Nonn, and G. Rempe, Nature (London) **395**, 33 (1998).

[12] T. J. Herzog, P. G. Kwiat, H. Weinfurter, and A. Zeilinger, Phys. Rev. Lett. **75**, 3034 (1995).

[13] L. Mandel, Rev. Mod. Phys. **71**, S274 (1999).

[14] S. Savasta, O. Di Stefano, V. Savona, and W. Langbein, Phys. Rev. Lett. **94**, 246401 (2005).

[15] M. O. Scully and K. Drühl, Phys. Rev. A **25**, 2208 (1982).

[16] H. Carmichael, *Statistical Methods in Quantum Optics I: Master Equations and Fokker-Planck Equations* (Springer, New York, 1999).

[17] H. J. Carmichael, R. J. Brecha, and P. R. Rice, Opt. Commun. **82**, 73 (1991).

[18] O. Di Stefano, A. Ridolfo, S. Portolan, and S. Savasta, Opt. Lett. **36**, 4509 (2011).

[19] A. P. Heberle, J. J. Baumberg, and K. Köhler, Phys. Rev. Lett. **75**, 2598 (1995).

[20] O. Di Stefano, R. Stassi, A. Ridolfo, S. Patanè, and S. Savasta, Phys. Rev. B **84**, 085324 (2011).

[21] J. Kasprzak, S. Reitzenstein, E. A. Muljarov, C. Kistner, C. Schneider, M. Strauss, S. Höfling, A. Forchel, and W. Langbein, Nat. Mater. **9**, 3304 (2010).

[22] J. McKeever, A. Boca, A. D. Boozer, J. R. Buck, and H. J. Kimble, Nature (London) **425**, 268 (2003).

[23] A. A. Abdumalikov, O. Astafiev, A. M. Zagoskin, Yu. A. Pashkin, Y. Nakamura, and J. S. Tsai, Phys. Rev. Lett. **104**, 193601 (2010).

[24] B. Peropadre, P. Forn-Diaz, E. Solano, and J. J. Garcia-Ripoll, Phys. Rev. Lett. **105**, 023601 (2010).

[25] A. Dousse, J. Suffczyński, A. Beveratos, O. Krebs, A. Lemaître, I. Sagnes, J. Bloch, P. Voisin, and P. Senellart, Nature (London) **466**, 217 (2010).

[26] S. Portolan, O. Di Stefano, S. Savasta, F. Rossi, and R. Girlanda, Phys. Rev. B **77**, 035433 (2008).

[27] S. De Liberato, D. Gerace, I. Carusotto, and C. Ciuti, Phys. Rev. A **80**, 053810 (2009).

[28] T. Niemczyk *et al.*, Nat. Phys. **6**, 772 (2010).

[29] I. Carusotto, S. De Liberato, D. Gerace, and C. Ciuti, e-print arXiv:1107.0445 (to be published).

[30] S. Savasta, R. Saija, A. Ridolfo, O. Di Stefano, P. Denti, and F. Borghese, ACS Nano **4**, 6369 (2010).

[31] A. Ridolfo, O. Di Stefano, N. Fina, R. Saija, and S. Savasta, Phys. Rev. Lett. **105**, 263601 (2010).

[32] J. Bochmann, M. Mucke, G. Langfahl-Klabes, C. Erbel, B. Weber, H. P. Specht, D. L. Moehring, and G. Rempe, Phys. Rev. Lett. **101**, 223601 (2008).